https://doi.org/10.5194/acp-2020-1110
Preprint. Discussion started: 6 November 2020

Atmospheric Chemistry and Physics Discussions

Co-emission of volcanic sulfur and halogens amplifies volcanic effective radiative forcing

John Staunton-Sykes[*1], Thomas J. Aubry[2,4], Youngsub M. Shin[1], James Weber[1], Lauren R. Marshall[1], Nathan Luke Abraham[1,3], Anja Schmidt[1,2], Alex Archibald[1,3]

[1]*Centre for Atmospheric Science, Department of Chemistry, University of Cambridge, Cambridge, UK*

[2]*Department of Geography, University of Cambridge, Cambridge, UK*

[3]*National Centre for Atmospheric Science, UK*

[4]*Sidney Sussex College, Cambridge, UK*

Correspondence to: J. Staunton-Sykes (email:jjas3@cam.ac.uk)

Abstract

The evolution of volcanic sulfur and the resulting radiative forcing following explosive volcanic eruptions is well understood. Petrological evidence suggests that significant amounts of halogens may be co-emitted alongside sulfur in some explosive volcanic eruptions, and satellite evidence indicates that detectable amounts of these halogens may reach the stratosphere. In this study, we confront an aerosol-chemistry-climate model with four stratospheric volcanic eruption emission scenarios (56 Tg SO_2 ± 15 Tg HCl & 0.086 Tg HBr and 10 Tg SO_2 ± 1.5 Tg HCl & 0.0086 Tg HBr) in order to understand how co-emitted halogens may alter the life cycle of volcanic sulfur, stratospheric chemistry and the resulting radiative forcing. The eruption sizes simulated in this work are hypothetical Volcanic Explosivity Index (VEI) 7 (e.g. 1257 Mt. Samalas) and VEI 6 (e.g. 1991 Mt. Pinatubo) eruptions, representing 1 in 500-1000 year and 1 in 50-100 year events respectively, with plausible amounts of co-emitted halogens based on satellite observations and volcanic plume modelling. We show that co-emission of volcanic halogens and sulfur into the stratosphere increases the volcanic ERF by 24 – 30% compared to sulfur-only emission. This is caused by an increase in both the forcing from volcanic aerosol-radiation interactions (ERF_{ari}) and composition of the stratosphere ($ERF_{clear,clean}$). Volcanic halogens catalyse the destruction of stratospheric ozone which results in significant stratospheric cooling (1.5 - 3 K); counteracting the typical stratospheric radiative heating from volcanic sulfate aerosol. The ozone induced stratospheric cooling prevents aerosol self-lofting and keeps the volcanic aerosol lower in the stratosphere with a shorter lifetime, resulting in reduced growth due to condensation and coagulation and smaller peak global-mean effective radius compared to sulfur-only simulations. The smaller effective radius found in both co-emission scenarios is closer to the peak scattering efficiency radius of sulfate aerosol, thus, co-emission of halogens results in larger peak global-mean ERF_{ari} (6 – 8%). Co-emission of volcanic halogens results in significant stratospheric ozone, methane and water vapour reductions, resulting in significant increases in peak global-mean $ERF_{clear,clean}$ (>100%), predominantly due to ozone loss. The dramatic global-mean ozone depletion simulated in both co-emission simulations (22%, 57%) would result in very high levels of UV exposure on the Earth's surface, with important implications for society and the biosphere. This work shows for the first time that co-emission of plausible amounts of volcanic

https://doi.org/10.5194/acp-2020-1110
Preprint. Discussion started: 6 November 2020

Atmospheric Chemistry and Physics Discussions

halogens can amplify the volcanic ERF in simulations of explosive eruptions; highlighting the need to include volcanic halogens fluxes when simulating the climate impacts of past or future eruptions and providing motivation to better quantify the degassing budgets and stratospheric injection estimates for volcanic eruptions.

1 Introduction

Sulfur gases emitted into the atmosphere by volcanic eruptions have a strong direct climate impact through the formation of sulfuric acid aerosol, which reflect incoming sunlight and cool the Earth's surface (Robock, 2000). Petrological data suggest that volcanic eruptions in some geological settings may also release substantial amounts of halogen gases into the atmosphere (Krüger et al., 2015; Kutterolf et al., 2013, 2015). Petrological analysis of the 1257 Mt. Samalas eruption suggests as much as 227 Tg of hydrogen chloride (HCl) and 1.3 Tg of hydrogen bromide (HBr) could have been emitted into the atmosphere alongside 158 Tg of sulfur dioxide (SO_2) (Vidal et al., 2016). The portion of the halogens erupted at the vent that reach the stratosphere is not well constrained and has been the subject of debate in the community for decades. Halogens are soluble (especially HCl) and may be scavenged by water, ice hydrometeors and ash in the volcanic plume (Halmer et al., 2002). Despite efficient scavenging, direct stratospheric injection of volcanic halogens is predicted by theory, and sophisticated plume models suggest that between 10% and 20% of the HCl emitted at the vent of large explosive eruptions could reach the stratosphere (Textor et al., 2003).

Aircraft measurements following the 2000 Mount Hekla eruption in Iceland showed that 75% of the HCl emitted at the vent entered the lower stratosphere and was still present 35 hours after the eruption suggesting that little scrubbing took place in the tropospheric eruption column (Hunton et al., 2005; Rose et al., 2006). Read et al., (2009) used retrievals from the Microwave Limb Sounder (MLS) to show that SO_2 and HCl was injected directly into the lower stratosphere during the 2004 Manam, 2007 Anatahan, 2008 Soufriere Hills, 2008 Okmok, 2008 Kasatochi, 2009 Redoubt, and 2009 Sarychev eruptions. Using retrievals from MLS, Prata et al., (2007) reported HCl at ~20 km in the volcanic plume of 2006 Soufriere Hills eruption plume, with stratospheric HCl:SO_2 gas ratios <0.1. Carn et al., (2016) reported MLS stratospheric HCl:SO_2 gas ratios of 0.01–0.03 (relative mixing ratios) for 14 small eruptions in the period between 2005 to 2014. Limitations with the field of view and spatial sampling of MLS mean these observed ratios are likely an underestimate (Carn et al,. 2016).

Petrological analysis in Bacon et al., (1992) suggested that the considerably larger, Volcanic Explosivity Index (VEI) 7, 7.6 kya eruption of Mt. Mazama degassed ~100 Tg of Cl, and the ice core record of the same eruption suggested 8.1 Tg Cl and 57.5 Tg SO_2 was injected into the stratosphere with a halogen injection efficiency of 8.1% and a stratospheric HCl:SO_2 molar ratio of ~0.3 (Zdanowicz et al., 1999). The two largest eruptions in the satellite era, 1982 El Chichón and 1991 Mt. Pinatubo, highlights the variability in stratospheric halogen injection following explosive volcanic eruptions. Both eruptions released relatively small amounts of halogens, 1.8 Tg (Varekamp et al., 1984) and 4.5 Tg of chlorine respectively with HCl:SO_2 molar ratios of ~0.4 (Mankin et al., 1992). Spectroscopic measurements made in the El Chichón stratospheric eruption plume indicated a local HCl increase of 40%, with a stratospheric injection of >0.04 Tg of HCl and a halogen injection efficiency of at least 2.5% (Mankin and Coffey, 1984, Woods et al., 1985). Woods et al., (1985) measured NaCl (halite) particles in the lower stratospheric eruption cloud of El Chichon derived from the chlorine-rich magma. They hypothesised

https://doi.org/10.5194/acp-2020-1110
Preprint. Discussion started: 6 November 2020

Atmospheric Chemistry and Physics Discussions

that the rapid ascent of large plinian eruption phases led to the formation of ice-bearing crystals and halite particles, which would lower the halogen scrubbing efficiency and preserve the halogens for stratospheric release. In the stratosphere, these halite particles may react with volcanic sulfuric acid leading to the formation of secondary HCl. In contrast, despite emitting more Cl into the atmosphere than El Chichón, observations following 1991 Mt. Pinatubo showed minimal stratospheric halogen injection as the halogens were more efficiently scavenged in the eruption cloud (Wallace and Livingston, 1992). The Pinatubo eruption occurred at the same time and location as a typhoon in the Philippines, and it is thought these very wet tropospheric conditions led to the effective wash out of halogens (McCormick et al., 1995, Self et al., 1996, Gerlach et al., 1996).

Overall, current datasets show that the stratospheric injection of volcanic halogens is highly variable and depends on both the total mass of halogens released at the vent and the degree of scavenging, determined by the geochemistry of the volcano and the prevailing atmospheric conditions during the eruption, particularly the humidity. It is clear, however, that volcanic halogens are injected into the stratosphere after some volcanic eruptions, and research into how these volcanic halogens may alter the volcanic aerosol microphysics, stratospheric chemistry, and the volcanic forcing is still limited.

Lurton et al. (2017) simulated the 2009 Sarychev Peak eruption (0.9 Tg) in The Whole Atmosphere Community Climate Model (WACCM) and showed how inclusion of halogens (27 Gg) allowed better agreement with modelled and observed data. Co-emission of halogens resulted in a lengthening of the SO_2 lifetime due to the further depletion of OH and a corresponding delay in the formation of aerosols with good agreement to in situ stratospheric measurements, showing how co-emitted halogens could impact volcanic sulfur processing.

Tie and Brasseur (1995) utilised model calculations to show how background atmospheric chlorine loadings altered the ozone response to volcanic sulfur injections. In conditions typical of the pre-1980 period, the ozone column abundance was shown to increase after a large volcanic eruption with the response being independent of the magnitude of the eruption. However, after 1980, higher background chlorine levels as a result of anthropogenic emissions of chlorofluorocarbons, meant that the ozone response became negative in winter at mid and high latitudes, with the magnitude of depletion increasing with eruption size. Since then, a number of prior studies have investigated the impact of volcanic halogens on stratospheric ozone. Cadoux (2015), petrologically determined chlorine and bromine degassing budgets for the Bronze Age Santorini eruption and, using a halogen injection efficiency of 2%, input 36 Tg S, 13.5 Tg of Cl and 0.02 Tg Br uniformly between the tropopause and 35 km in a pre-industrial background state within a 2D chemical transport model (CTM). They simulated ozone depletion lasting a decade with a peak global-mean of 20-90% over the NH. The stratospheric injection HCl:SO_2 molar ratio of 0.64 is considerably larger than observations from MLS (<0.1) and ice core records of Mount Manzana (<0.3). Klobas et al., 2017, also used a 2D CTM to study the impact that co-emission of volcanic halogens has on column ozone in contemporary and future background states. They simulated hypothetical Pinatubo sized eruptions with stratospheric injection HCl:SO_2 mixing ratio of ~0.14, and reported global ozone depletion lasting ~2-3 years with a peak of 20%. These CTM studies used prescribed wind fields and, as a result, do not include the important interactive feedbacks of radiation and dynamics which alter the transport of tracers and thus the composition of the atmosphere. Ming et al., (2020) simulated explosive tropical eruptions in the UM-UKCA interactive

https://doi.org/10.5194/acp-2020-1110
Preprint. Discussion started: 6 November 2020

Atmospheric Chemistry and Physics Discussions

stratospheric aerosol model and found that a volcanic halogen emission of 0.02 Tg ($HCl:SO_2$ = 0.04) into a pre-industrial background state had little impact on column ozone but 2 Tg ($HCl:SO_2$ = 0.4) showed significant and prolonged ozone depletion above both poles. Brenna et al., (2019), used CESM1(WACCM) with prescribed volcanic aerosols and SSTs to simulate an average eruption of a Central American Volcanic Arc volcano in a pre-industrial background state, with a 10% halogen injection efficiency (2.5 Tg Cl, 9.5 Gg Br). They found ozone depletion of up to 20% globally for 10 years, with ozone hole conditions over the tropics and Antarctica. Consequently, UV radiation increases of >80% were simulated for 2 years. These studies did not, however, investigate how volcanic halogens may interact with the sulfur aerosol life cycle and interact to modulate volcanic forcing. Brenna et al (2020) used Community Earth System Model 2 (WACCM6) to investigate the coupling and feedback between volcanic aerosol, chemistry, radiation and climate pre-industrial background state. They investigate the combined effect of the sulfur (523 Tg S) and halogens (120 Tg Cl, 0.2 Tg Br) emissions of the Los Chocoyos supereruption assuming a 10% halogen injection efficiency and stratospheric $HCl:SO_2$ molar ratio ~0.4, on volcanic gases, ozone and surface UV. Compared to simulations with sulfur-only injections, they simulate a lower peak sulfate burden attributed to the delay in SO_2 oxidation but with the same total sulfur lifetime and aerosol effective radius. Thus, the co-emission of halogens results in a smaller radiative forcing, 20% lower compared to sulfur-only.

Very recently Wade et al. (2020) compared HadGEM3-ES simulations of the 1257 Mt. Samalas eruption, utilising the halogen degassing estimates from Vidal et al. (2016) and stratospheric halogen injection efficiencies of 20% and 1%, with the available surface temperature proxies. Their results suggest it is unlikely that 20% of degassed halogens reached the stratosphere, however smaller fractions gave good agreement with multi-proxy records

The aim of this study is to confront a coupled chemistry-aerosol model with hypothetical VEI 6 and VEI 7 sized eruptions, both with and without halogens, and investigate how the co-emission of volcanic sulfur and halogens alters the evolution of volcanic aerosol, ozone, stratospheric composition, and the consequential radiative forcing and UV flux.

2 Data and Methods

2.1 Model Description

This study utilises the coupled aerosol-chemistry-climate model consisting of the United Kingdom Chemistry and Aerosol (UKCA) module together with the UK Met Office Unified Model (UM). The UKCA module is run at UM version 11.2 with the combined stratosphere and troposphere chemistry (StratTrop) scheme (Archibald et al 2020). The model is free-running in the atmosphere, forced by surface boundary conditions (sea ice and sea surface temperatures), similar to the UK Earth system model (UKESM1) Atmospheric Model Intercomparison Project (AMIP) simulation submitted to the Coupled Model Intercomparison Project Phase 6 (CMIP6) (Sellar et al., 2019, Sellar et al.,2020). The resolution was 1.875° longitude by 1.25° latitude with 85 vertical levels extending from the surface to 85 km. The dynamics of the stratosphere have previously been shown to be well represented in this model, and it has an internally generated Quasi-Biennial Oscillation QBO (Osprey et al., 2013). The model includes the fully interactive stratospheric GLOMAP-mode aerosol scheme which simulates microphysical

https://doi.org/10.5194/acp-2020-1110
Preprint. Discussion started: 6 November 2020

Atmospheric Chemistry and Physics Discussions

processes including the formation, growth, transport and loss of aerosol (Dhomse et al., 2014). GLOMAP-mode also calculates aerosol optical properties online which are used to calculate direct and indirect radiative effects (Mulcahy et al., 2020).

In UKCA, stratospheric ozone concentrations are determined by sets of photochemical reactions as well as ozone destroying catalytic cycles involving chlorine, bromine, nitrogen, and hydrogen radical species (Archibald, 2020). Photolysis reactions in UKCA utilise rates calculated from a combination of the FAST-JX scheme and look-up tables (Telford et al., 2013). Ozone depleting radical species are produced by the photolysis of halogen containing compounds reacting on the surface of stratospheric aerosols, including hydrochloric acid (HCl), chlorine nitrate ($ClONO_2$), hydrogen bromide (HBr), and bromine nitrate ($BrONO_2$). Heterogeneous reactions in the presence of polar stratospheric clouds (PSCs) in the polar lower stratosphere or in the presence of sulfate aerosol following explosive volcanic eruptions are also important for stratospheric ozone concentrations. Eight additional heterogeneous reactions involving chlorine and bromine species were added as described in Ming et al., (2020), with the main change being the explicit treatment of the reactions of four additional chemical species: Cl_2, Br_2, $ClNO_2$, and $BrNO_2$ which are photolysed to produce Cl and Br radicals.

Volcanic effective radiative forcings (hereafter ERF) are calculated as differences (Δ) in the net top of atmosphere (TOA) radiative fluxes (F) between perturbed and control simulations, as follows:

$$ERF = \Delta F$$

Volcanic ERF is decomposed as described in Schmidt et al., (2018) and Ghan (2013), as follows:

$$ERF = \Delta(F - F_{clean}) + \Delta\left(F_{clean} - F_{clear,clean}\right) + \Delta F_{clear,clean}$$

$$= ERF_{ari} + ERF_{aci} + ERF_{clear,clean}$$

This decomposition is enabled by implementing extra calls to the radiation scheme as recommended by Ghan (2013) to obtain F_{clean} and $F_{clear,clean}$. Where F_{clean} denotes a radiation flux diagnostic calculation without aerosol-radiation interactions but including aerosol-cloud interactions through microphysics. $F_{clear,clean}$ denotes a radiation flux diagnostic calculation that ignores both aerosol and cloud-radiation interactions. Thus, $F - F_{clean}$, determines the impact of all aerosols and $\Delta(F - F_{clean})$ is an estimate of the forcing from volcanic aerosol-radiation interactions (ERF_{ari}). The second term $\Delta(F_{clean} - F_{clean,clear})$ represents the difference in the clean-sky cloud radiative forcing, and is an estimate of the aerosol-cloud interactions (ERF_{aci}) due to volcanic emissions. The third term, $ERF_{clear,clean}$ accounts for changes not directly due to aerosol or cloud interactions, largely the result of changes in surface albedo and atmospheric composition. In this study, we fix surface temperature and sea-ice fields meaning that surface albedo is expected to be unchanged and any $F_{clear,clean}$ changes are the result of atmospheric compositional changes.

https://doi.org/10.5194/acp-2020-1110
Preprint. Discussion started: 6 November 2020

Atmospheric Chemistry and Physics Discussions

2.2 Experimental Design

We utilise atmosphere-only, time-slice experiments whereby the initial sea surface temperature, sea ice fraction and forcing agents are prescribed climatologies with values taken from fully coupled UKESM1.0 historical runs produced for CMIP6 (Eyring et al. 2016) and averaged over the years 1990 - 2000. The 1990s, and thus these timeslices, were characterised by high background halogen levels due to anthropogenic emissions of CFCs throughout the preceding decade. A control simulation was run with a 15 year spin up followed by a further 20 years. The effect of explosive volcanic eruptions was investigated by running a series of 10 year volcanic perturbations spun off from 6 different years in the control run to represent the variability in QBO states. Changes are plotted as the difference between the average of the 6 ensembles and the climatology derived from the 20 year control run, cumulative forcings are calculated as the sum of the forcing over the full 10 year simulation duration. The volcanic emissions are prescribed by direct injection of SO_2, HCl and HBr into the stratosphere with a Gaussian plume vertical distribution centred on 21 km, lasting for 24 hours on July 1st. The gases were injected in the tropics (5ºS latitude and 0º longitude) to represent a typical tropical explosive eruption (Newhall et al., 2017).

Since historical stratospheric volcanic SO_2 fluxes are variable and the volcanic flux of HCl and HBr into the stratosphere remains uncertain, we developed a simulation matrix that spans a range of possible explosive volcanic emissions. The four sets of experiments have one high SO_2 (56 Tg), and one low SO_2 (10 Tg) emission scenario both with (HAL56 and HAL10) and without halogens (SULF56 and SULF10), as shown in Table 1. These eruption sizes (56 and 10 Tg SO_2) are similar in size to a VEI 7 (e.g. 1257 Mt. Samalas) and VEI 6 (e.g. 1991 Mt. Pinatubo) eruption, representing 1 in 500 -1000 year and 1 in 50-100 year events respectively. HAL56 utilises the 1257 Mt. Samalas HCl and HBr emission estimates from Vidal et al. (2014) and assumes a conservative ~5% stratospheric halogen injection efficiency, less than the 10-20% predicted by plume modelling in Textor et al (2013) and closer to the observed efficiency following El Chichon (>2.5%) and in the ice core record of Mt. Mazama (8%), as well as the fraction supported by Wade et al. (2020). This results in a HCl:SO_2 molar ratio of ~0.47, similar to the ratios simulated in Ming et al., 2020, and Brenna et al., 2020 and smaller than the ratio simulated in Cadoux et al., 2015. HAL10 has a SO_2 injection similar to 1991 Pinatubo and a 10 times smaller flux of HCl and HBr than HAL56, resulting in a HCl:SO_2 molar ratio of ~0.26, very close to the estimated stratospheric injection ratio for Mt. Mazama (0.3) (Zdanowicz et al., 1999).

Scenario	SO_2 (Tg)	HCl (Tg)	HBr (Tg)	HCl:SO_2 (molar ratio)
SULF56	56	-	-	-
HAL56	56	15	0.086	0.47
SULF10	10	-	-	-
HAL10	10	1.5	0.0086	0.26

https://doi.org/10.5194/acp-2020-1110
Preprint. Discussion started: 6 November 2020

Atmospheric Chemistry and Physics Discussions

Table 1 Showing the eruption masses of SO2, HCl and HBr in Tg for the four sets of experiments. Equivalent effective Stratospheric Chlorine (EESC) = [Cl] added to stratosphere+ 60 × [Br] added to stratosphere (Cadoux et al., 2015).

3 Results

3.1 Sulfur Microphysics and ERF_{ari}

Atmospheric burdens of volcanic sulfur species are summarized in Figure 1. As found by Lurton et al., (2017), volcanic halogens deplete OH via equation 1

$$HCl + OH \rightarrow Cl + H_2O \qquad Eq.1$$

which limits the availability of OH for SO_2 oxidation, leading to slower destruction of volcanic SO_2 and an increase in SO_2 e-folding time of 21% and 40% in HAL10 and HAL56 compared to SULF10 and SULF56 respectively. As the rate of formation of sulfuric acid is decreased, we simulate a corresponding delay in the formation in sulfate aerosol and a reduction in the peak sulfate aerosol burden by 8% in both HAL10 and HAL56.

https://doi.org/10.5194/acp-2020-1110
Preprint. Discussion started: 6 November 2020

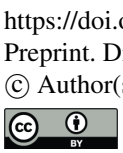

Atmospheric Chemistry and Physics Discussions

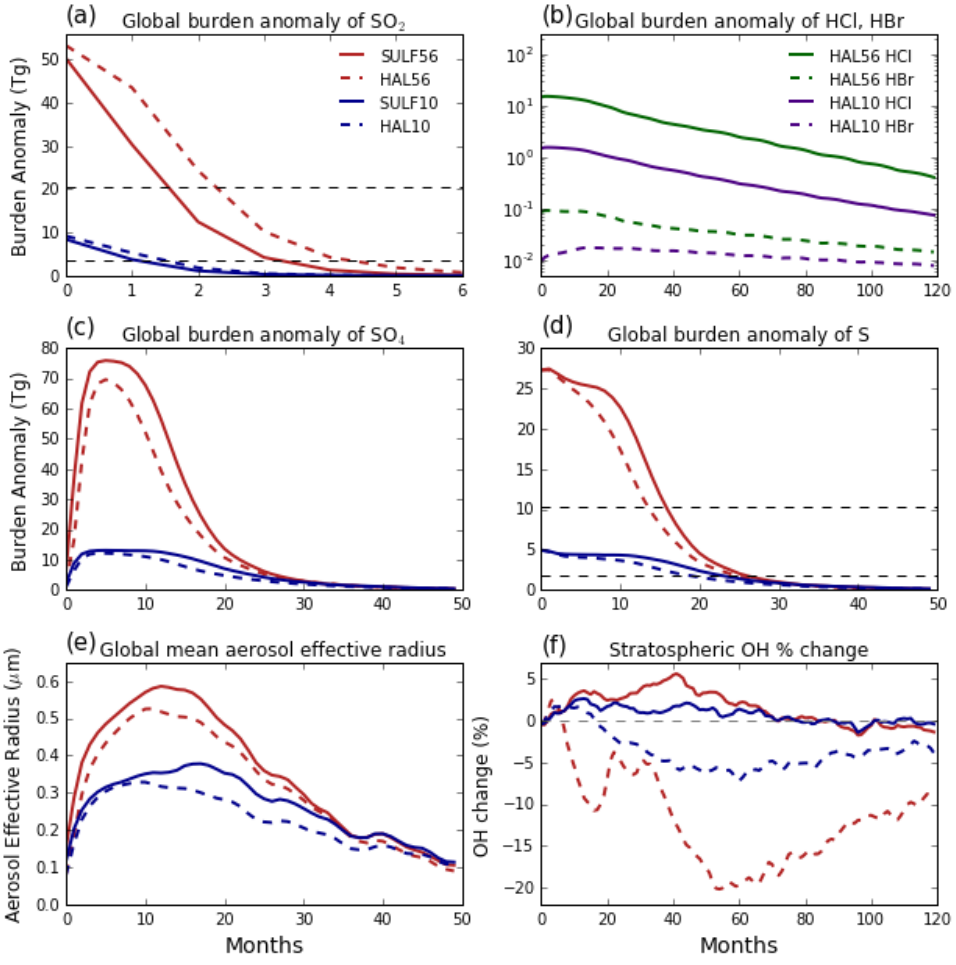

Figure 1 - Global evolution of sulfur, halogens and OH for the SULF56, HAL56, SULF10 and HAL10 simulations. **(a)** SO_2 burden anomalies. **(b)** HCl and HBr burden anomalies on log scale. **(c)** Sulfate aerosol burden anomalies. **(d)** Total sulfur burden anomalies. (e) Global-mean aerosol effective radius, weighted by aerosol surface area density. **(f)** Stratospheric OH change (%). Dashed horizontal lines in (a) (b) and (d) represent 1/e. Note the different axis scales.

Despite the slower rate of SO_2 oxidation, the co-emission of halogens reduces the lifetime of the sulfur burden to 17.3 and 11.7 months in HAL10 and HAL56, compared with 21.2 and 13.6 months in SULF10 and SULF56, a decrease of 18% and 14% respectively. This indicates that co-emission of halogens alters the rate at which sulfur is removed from the atmosphere. Significant differences in temperature change are simulated between the sulfur-only and halogen simulations. In sulfur-only simulations, strong positive temperature anomalies of ~3 K due to sulfate aerosol absorption of infra-red radiation are simulated across the tropical stratosphere (Figure 2). This aerosol heating lofts volcanic aerosol to altitudes higher than the initial injection height in the model. By contrast, co-emission of volcanic halogens results in significant stratospheric ozone depletion of 22-57% (see section 3.2)

https://doi.org/10.5194/acp-2020-1110
Preprint. Discussion started: 6 November 2020

Atmospheric Chemistry and Physics Discussions

and in turn this results in large negative temperature anomalies over most of the lower and middle stratosphere ~ -3 K (Figure 2). Ozone generates heat in the stratosphere by absorbing both incoming SW radiation from the sun and by absorbing upwelling LW radiation from the troposphere. Thus, decreasing stratospheric ozone results in lower stratospheric temperatures; the effect of which is larger in magnitude than the aerosol heating and prevents volcanic sulfate aerosol being self-lofted. The volcanic sulfate aerosol thus remains at significantly lower altitudes in HAL10 and HAL56 (~21-22km) compared with SULF10 and SULF56 (~24-25km) (Figure 2). Lower altitude aerosol remains in a faster branch of the Brewer-Dobson Circulation (Figure S1) which results in faster transport to high-latitudes and removal from the stratosphere (Figure 1d).

https://doi.org/10.5194/acp-2020-1110
Preprint. Discussion started: 6 November 2020

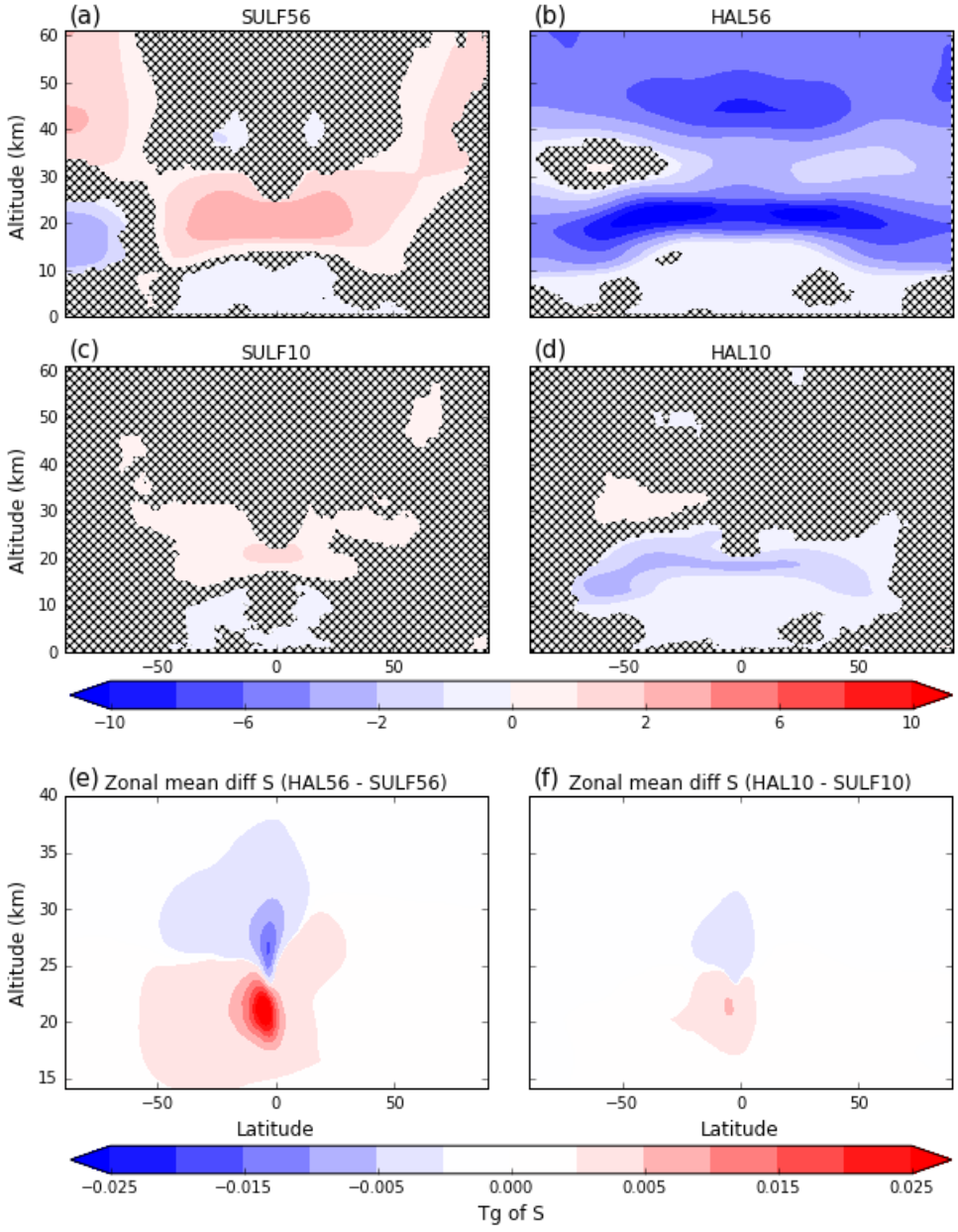

Figure 2 Zonal mean temperature difference averaged over the first 3 years post eruption. **(a)** SULF56, **(b)** HAL56, **(c)** SULF10, **(d)** HAL10. Zonal difference in sulfur burden averaged over the first 2 years post eruption **(e)** HAL56 -SULF56, **(f)** HAL10 - SULF10. Differences that are not significant at the 95% confidence interval according to a Mann–Whitney U test are indicated with stipples.

https://doi.org/10.5194/acp-2020-1110
Preprint. Discussion started: 6 November 2020

Atmospheric Chemistry and Physics Discussions

The shorter lifetime of sulfur in the atmosphere following HAL10 and HAL56 eruptions results in stunted aerosol growth and smaller aerosol effective radii (R_{eff}). Peak global-mean R_{eff} is ~15% and ~10% smaller in HAL10 and HAL56 compared to their equivalent SULF simulations (Figure 1e). This aerosol growth stunting effect is a direct result of the shorter sulfur lifetime, rapid spreading and removal of aerosol. Volcanic sulfate aerosols grow through microphysical processes of condensation and coagulation (Kremser et al., 2016). The faster removal of sulfate aerosol in HAL10 and HAL56 reduces the growth via condensation and coagulation and results in smaller peak global-mean aerosol R_{eff}. This theory is supported by Figure 3 which shows a scatter plot of 3-year global-mean aerosol effective radius as a function of the global sulfur burden e-folding time with a significant correlation within both 10 Tg (r=0.88) and 56 Tg (r=0.95) eruption ensembles. The positive correlation between these two variables holds only for each eruption size scenario. The larger SO_2 injection in HAL56 and SULF56 leads to larger-sized sulfate aerosols, faster sedimentation and shorter removal time compared to HAL10 and SULF10, as seen by comparing Figures 3a and 3b.

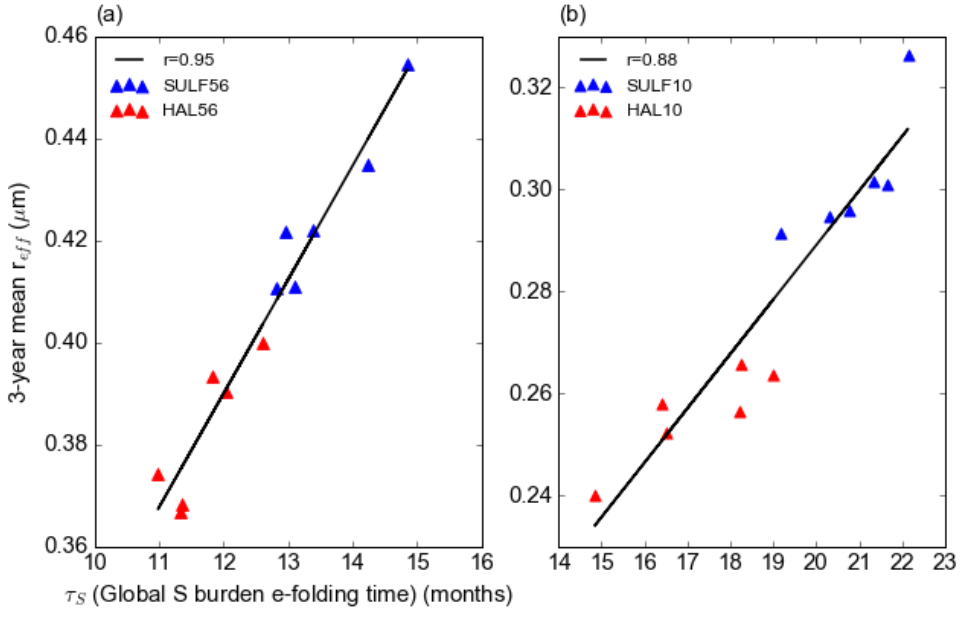

Figure 3 Global-mean aerosol effective radius over the first 3 post eruption years as a function of the global total sulfur e-folding time. **(a)** SULF56 and HAL56, **(b)** SULF56 and HAL56. Both plots have regression lines fitted with correlation coefficient (r) showing strong positive correlation.

The radiative impact of sulfate aerosols depends on the particle size (Timmreck et al., 2010). Using Mie scattering theory, Lacis (2015) found that the cross section per unit mass is largest for sulfate aerosol with effective radius of ~0.25 μm. The smaller R_{eff} in HAL10 and HAL56 is closer to 0.25μm and results in more efficient scattering of radiation per unit mass (Timmreck, 2012). Therefore, we simulate 11% and 22% higher peak global-mean stratospheric aerosol optical depth (SAOD) anomalies in HAL10 and HAL56 than their equivalent SULF

https://doi.org/10.5194/acp-2020-1110
Preprint. Discussion started: 6 November 2020

Atmospheric Chemistry and Physics Discussions

simulations (Figure 4), despite having a 14% and 9% smaller peak aerosol burden. Correspondingly, we simulate an 8% and 6% increase in the peak global-mean ERF_{ari} in HAL10 and HAL56 compared to SULF10 and SULF56 (Figure 4). The SAOD and ERF_{ari} anomalies are a balance between the offsetting effects of smaller aerosol and shorter lifetime which result in a net-zero impact on cumulative ERF_{ari} despite a significant increase in the peak global-mean ERF_{ari} (Figure S2a,b).

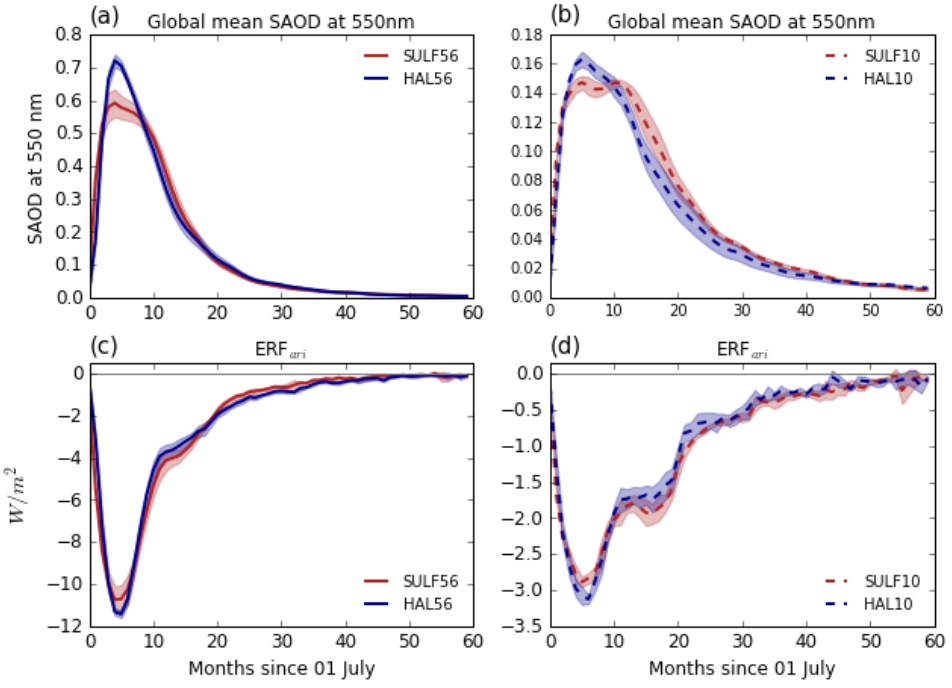

Figure 4 Global-mean evolution of SAOD anomaly at 550nm, **(a)** SULF56 and HAL56, **(b)** SULF10 and HAL10. Global-mean evolution of top of atmosphere global-mean ERF_{ari} **(c)** SULF56 and HAL56, **(d)** SULF10 and HAL10..

3.2 Composition Changes and Resulting $ERF_{clear,clean}$

Co-emission of volcanic sulfur and halogens causes significant perturbations to the chemistry of the stratosphere beyond the depletion of OH in HAL10 and HAL56 mentioned in section 3.1 Stratospheric methane, stratospheric water vapour (SVW) and, in particular, stratospheric ozone are all impacted.

In sulfur-only simulations, we simulate a modest reduction in global-mean ozone column, -9 DU (-3.9%) in SULF10 and -15 DU (-6.6%) in SULF56 (Figure 5a,c). This ozone depletion is catalysed by halogen radicals activated from background halogens on the surface of volcanic aerosol. In simulations with co-emitted halogens we simulate more dramatic ozone depletions; HAL10 resulted in a peak global-mean ozone reduction of 65 DU (-22%) 1-2 years after the eruption followed by a gradual recovery over the next 3-4 years (Figure 5d). HAL56

https://doi.org/10.5194/acp-2020-1110
Preprint. Discussion started: 6 November 2020

Atmospheric Chemistry and Physics Discussions

resulted in a peak global-mean ozone reduction of 175 DU (-57%) 1-2 years after the eruption followed by a gradual recovery the remainder of the 10 year simulation, with an average reduction of 82 DU (-27%) over the 10 year simulation (Figure 5b).

Volcanic halogen catalysed ozone depletion was simulated across all latitudes, but the largest magnitude changes in HAL10 (-40%) and HAL56 (-80%) were within the aerosol cloud and the polar regions, where the co-emitted halogens were activated on aerosol surfaces and PSCs respectively (Figure 5). In both HAL10 and HAL56 tropical ozone was found to recover first with significant depletions recurring during the winter in the polar regions for the remainder of the simulation. Ozone depletion shows a similar bimodal altitude distribution in the stratosphere similar to that found in Brenna et al., (2020), with 3 year mean depletion maxima (-1 ppmv and -3.5 ppmv in HAL10 and HAL 56) in the lower (20 km) and upper (40km) stratosphere (Figure 6).

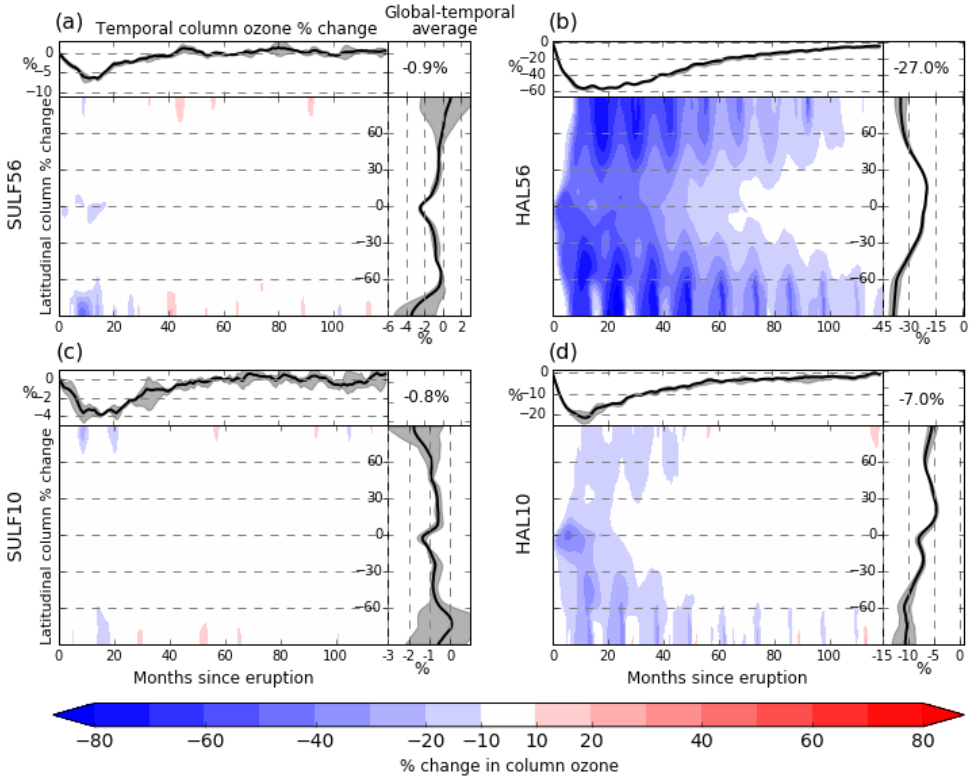

Figure 5 Ozone% difference in response to the simulated volcanic eruptions **(a)** SULF56, **(b)** HAL56, **(c)** SULF10, **(d)** HAL10. Global averages of total column ozone perturbation are traced atop each panel as a function of time. Temporal average ozone anomalies are traced right, note different scales. Global-temporal averages are enumerated in the top right. Red colors indicate column ozone enhancement, and blue colors indicate column ozone depletion.

https://doi.org/10.5194/acp-2020-1110
Preprint. Discussion started: 6 November 2020

Atmospheric Chemistry and Physics Discussions

Following sulfur-only eruptions we simulate small enhancements in stratospheric water vapour (SWV) and methane (Figure 8). SULF10 results in a peak increase in SWV of 0.4 ppmv (+7%) and a 10 ppbv (0.8%) increase in stratospheric methane 3-4 years after the eruption. SULF56 results in a peak increase in SWV of 1.1 ppmv (+17%) and a 30 ppbv (2.5%) increase in stratospheric methane 3-4 years after the eruption, perturbations recover gradually over the remainder of the simulation. Unlike in sulfur-only eruptions, following eruptions with co-emitted halogens we simulate a reduction in SWV and methane (Figure 8). HAL10 and HAL56 result in a peak SWV reduction of 1.0 ppmv (-16%) and 2.3 ppmv (-36%) respectively 3-4 years after the eruption followed by a gradual recovery. In HAL10 SWV perturbation levels return to the background levels over 6-7 years whereas in HAL56 the perturbation does not fully recover within the 10 year duration of the simulation. HAL10 and HAL56 result in a peak mean stratospheric methane reduction of 37 ppbv (-3%) and 214 ppbv (-18%) respectively 2 years after the eruption. In HAL10 the stratospheric methane perturbation returns to the background levels over 3-4 years whereas in HAL56 the perturbation remains below zero for between 7-8 years.

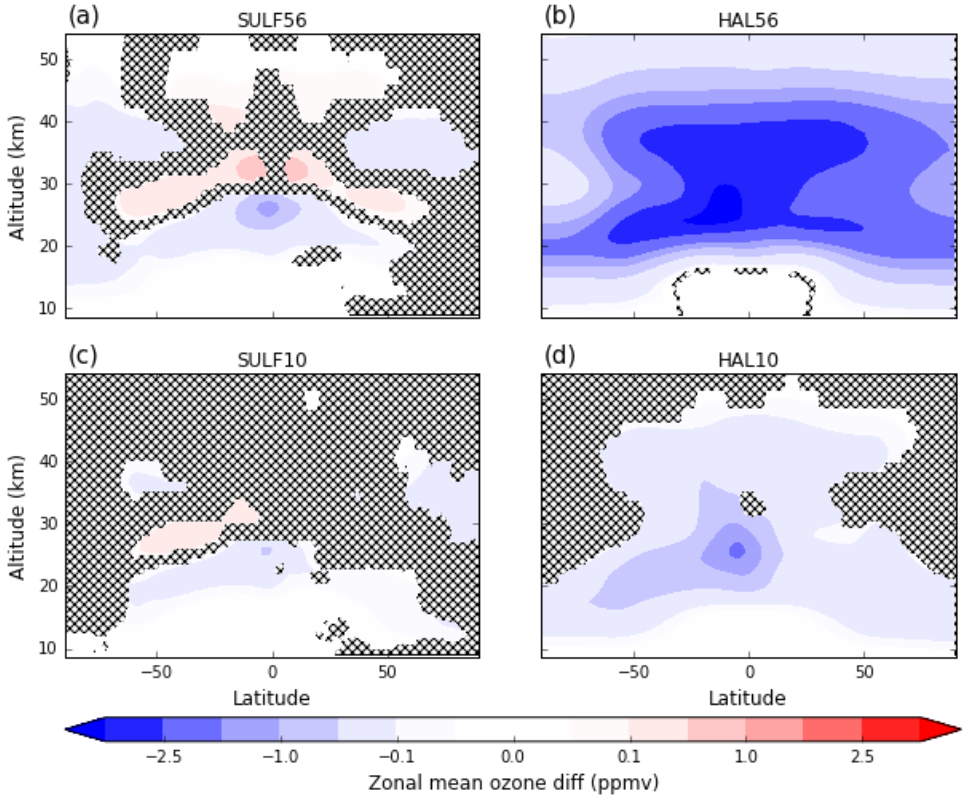

Figure 6 Zonal mean difference in ozone (ppmv) averaged over the first 3 years post eruption, **(a)** SULF56, **(b)** HAL56, **(c)** SULF10, **(d)** HAL10. Red colors indicate ozone enhancement, and blue colors indicate ozone depletion. Differences that are not significant at the 95% confidence interval according to a Mann–Whitney U test are indicated with stipples.

https://doi.org/10.5194/acp-2020-1110
Preprint. Discussion started: 6 November 2020

Atmospheric Chemistry and Physics Discussions

Stratospheric SWV and methane levels are linked. SWV has two main sources: transport from the troposphere and, chemical production from methane (Loffler et al., 2016). Whereas, as well as being oxidised by OH to form SWV, stratospheric methane is also destroyed by reaction with halogens via equation 2 and is sourced mainly from transport from the troposphere.

$$Cl. + CH_4 \rightarrow HCl + CH_3 \qquad Eq. 2$$

Sulfur-only eruptions cause an increase in the levels of stratospheric methane, in agreement with Loffler et al. (2015), who showed stratospheric methane mixing ratios increased by ~5% following simulations of El Chichon and 15-20% following the larger Mt Pinatubo. They showed that major volcanic eruptions do not increase the upward transport of methane from the troposphere to the stratosphere, but rather, the increased stratospheric methane levels are due to lengthening of stratospheric methane lifetime. When we co-emit halogens, enhanced destruction of methane by chlorine via Eq 2 results in the significant decrease in the HAL10 and HAL56 stratospheric methane levels.

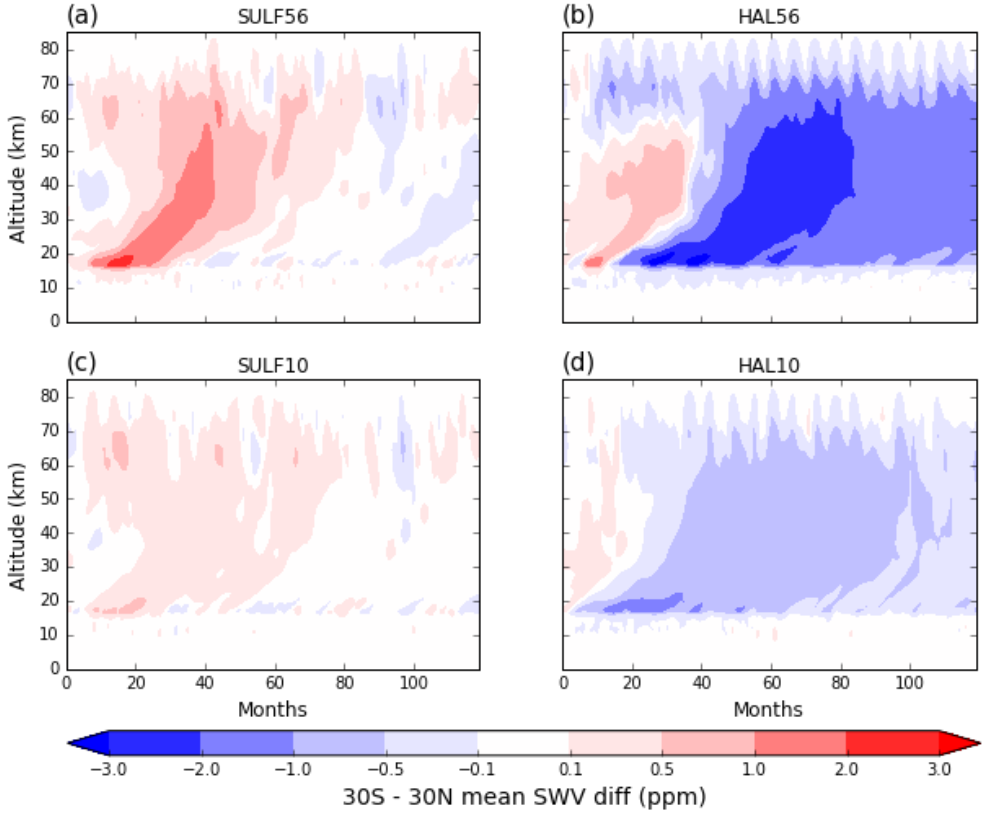

https://doi.org/10.5194/acp-2020-1110
Preprint. Discussion started: 6 November 2020

370 **Figure 7** 30°S - 30°N Mean difference in SWV (ppmv) as a function of altitude and time, **(a)** SULF56, **(b)** HAL56, **(c)** SULF10, **(d)** HAL10. Red colors indicate SWV enhancement, and blue colors indicate column ozone depletion.

The simulated changes in methane are small in comparison to the SWV changes across all simulations and thus
375 can only account for a fraction of the SWV change. Both with and without halogens, the dominant driver of SWV change is the amount of water vapour entering the stratosphere through the tropical tropopause (Loffler et al., 2016). SULF10 and SULF56 resulted in elevated SWV as volcanic aerosol heating lead to more air being brought from the troposphere and a weakening of the tropical tropopause cold trap dehydration effect (Figure 8) (Loffler et al., 2016). Elevated SWV is seen to initiate at the tropical troposphere before spreading higher into the
380 stratosphere (Figure 7a,c). In the case of co-emitted halogens, the process is the same but in the opposite sense. Cooling in the tropical tropopause vicinity reduces the amount of water vapour being brought up from the troposphere and increases the efficiency of the tropical cold trap dehydration effect (Figure 8) (Loffler et al., 2016). The negative SWV anomalies can be seen to initiate at the troposphere before spreading higher into the stratosphere (Figure 7b,d).

385

https://doi.org/10.5194/acp-2020-1110
Preprint. Discussion started: 6 November 2020

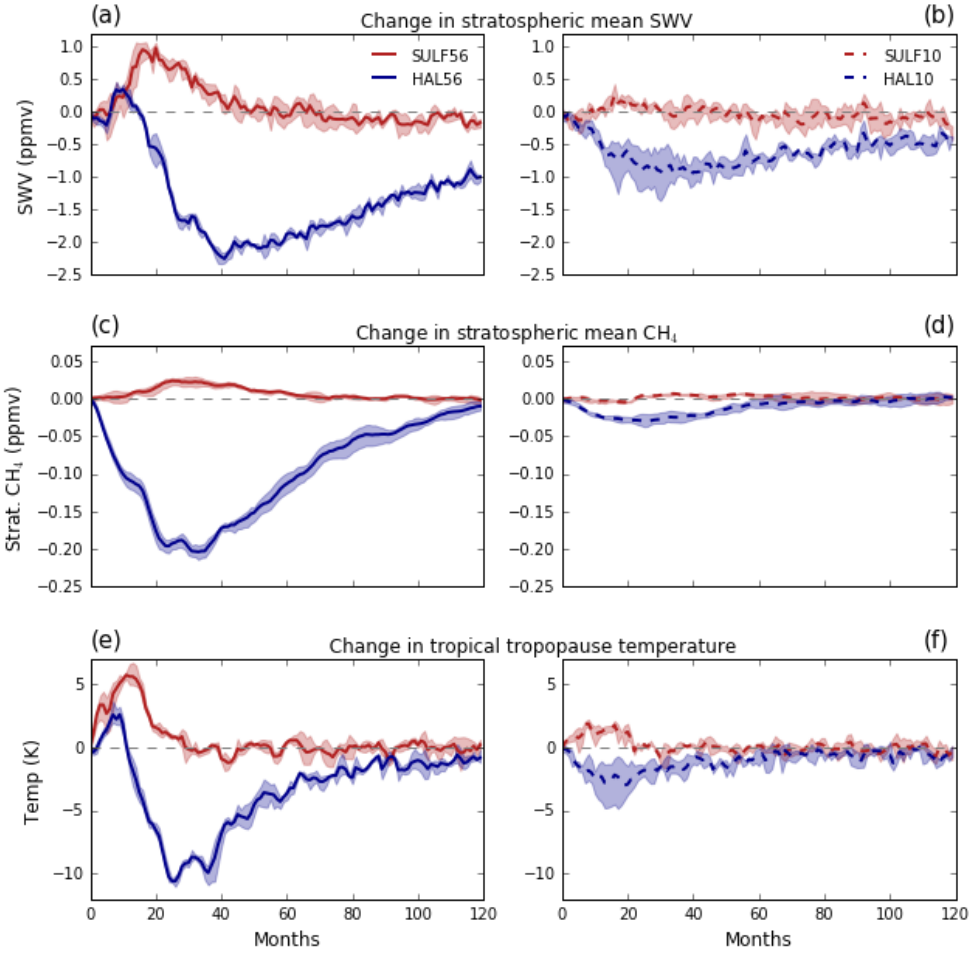

Figure 8 Evolution of stratospheric mean water vapour (ppmv) in SULF56 and HAL56 **(a)**, and SULF10 and HAL10 **(b)**.Evolution of stratospheric methane (ppmv) in SULF56 and HAL56 **(c)**, and SULF10 and HAL10 **(d)**. Evolution of tropical tropopause cold trap temperature difference averaged over 30S - 30N and 15-20km in SULF56 and HAL56 **(e)**, and SULF10 and HAL10 **(f)**.

Using the forcing diagnosis outlined in Schmidt et al., (2018) and Ghan (2013), we can isolate the radiative forcing due to atmospheric composition and surface albedo changes, $ERF_{clear,clean}$. As we prescribe surface temperature and sea ice, surface albedo changes are assumed to be unchanged, meaning that $ERF_{clear,clean}$ represents the forcing from atmospheric composition changes (Figure 9 c, d). HAL10 results in a peak global-mean $ERF_{clear,clean}$ of -1.3 Wm^{-2} one year after the eruption, more than double the $ERF_{clear,clean}$ of SULF10. The forcing recovers gradually over the next 6-7 years and results in a cumulative $ERF_{clear,clean}$ that is 5 times greater than SULF10 (Figure S2d). Similarly, HAL56 results in a peak global-mean $ERF_{clear,clean}$ of -2.1 Wm^{-2} 1-2 years after the eruption, double the peak global-mean forcing of SULF56. The $ERF_{clear,clean}$ anomaly in HAL56 is more persistent and remains -0.5

https://doi.org/10.5194/acp-2020-1110
Preprint. Discussion started: 6 November 2020

Atmospheric Chemistry and Physics Discussions

Wm^{-2} below zero at the end of the 10 simulation, resulting in a cumulative $ERF_{clear,clean}$ that is 10 times greater than SULF56 (Figure S2c).

Using the whole atmosphere ozone radiative kernel from Rap et al., 2015, we are able to show that the stratospheric ozone change is the dominant driver of the $ERF_{clear,clean}$ accounting for ~75% of the $ERF_{clear,clean}$ (Figure 9 a,b). The remainder is likely predominantly due to SWV changes with a small contribution from stratospheric methane changes. The latitudinal pattern of ozone radiative forcing reflects the locations of the ozone change, with largest forcings at the poles.

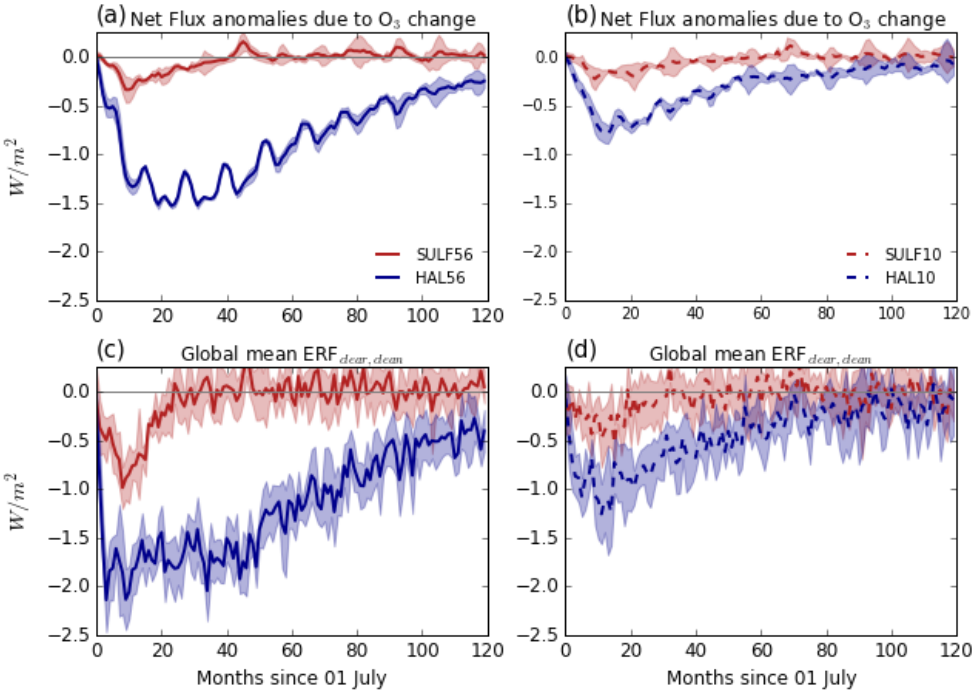

Figure 9 Evolution of global-mean TOA net flux anomalies due to stratospheric O_3 change, in SULF56 and HAL56 estimated from the ozone radiative kernel from Rap et al. (2015) **(a)**, SULF10 and HAL10 **(b).** Evolution of the global-mean top of atmosphere compositional forcing ($ERF_{clear,clean}$) in SULF56 and HAL56 **(c)**, SULF10 and HAL10 **(d)** Ozone changes make up ~75% of the $ERF_{clear,clean}$.

4 Discussion

Using the Ghan (2013) method for diagnosing forcing, we have shown that the co-emission of volcanic halogens results in larger peak global-mean ERF_{ari} and $ERF_{clear,clean}$. Taking these in combination, the co-emission of halogens results in substantial increases in the peak global-mean volcanic ERF to -4.1 Wm^{-2} (+30%) in HAL10, and -14.1 Wm^{-2} (+24%) in HAL56 (Figure 10a,b), as well as increases in the total cumulative forcing to -1.37 x10^{23} J (+60%) in HAL10 and -3.86x10^{23} J (+100%) in HAL56 compared to SULF10 and SULF56 (Figure S2e,f).

https://doi.org/10.5194/acp-2020-1110
Preprint. Discussion started: 6 November 2020

Atmospheric Chemistry and Physics Discussions

In both HAL10 and HAL56, ~25% of the additional peak global-mean volcanic ERF simulated compared to SULF10 and SULF56 respectively comes from the changes to the ERF_{ari}, with the remainder coming from changes to $ERF_{clear,clean}$.

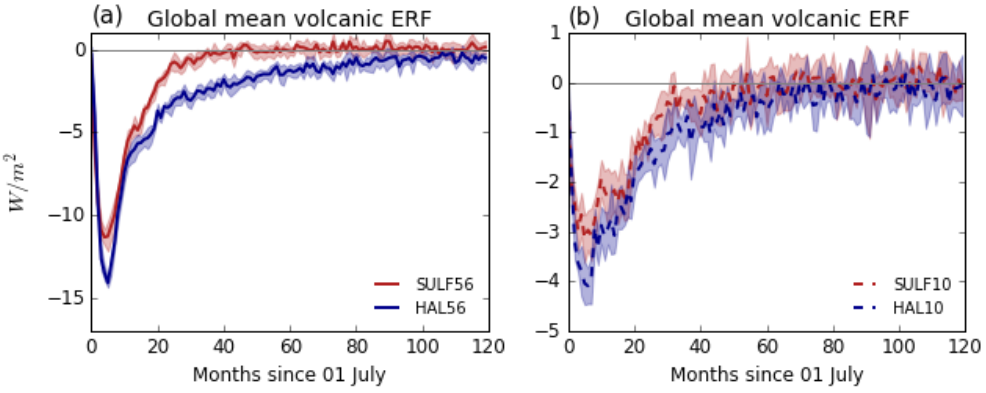

Figure 10 Evolution of the global-mean top of atmosphere total volcanic forcing ERF forcing (volcanic ERF) in SULF56 and HAL56 **(a)**, SULF10 and HAL10 **(b).** Volcanic ERF is the sum of ERF_{ari} , ERF_{acii} and $ERF_{clear,clean}$.

Comparing the perturbations in HAL56 to HAL10, we find that increasing the volcanic halogen flux by 10 times only results in a ~2.5 times larger global ozone response and, as $ERF_{clear,clean}$ is dominated by changes in stratospheric ozone, only a ~2 times larger $ERF_{clear,clean}$. This suggests that there is a saturation in the ozone depleting potential of co-emitted volcanic halogens. Plotting the column ozone percentage change against the injected Equivalent Effective Stratospheric Chlorine (EESC) from this study and a number of previous studies, we find an exponential decay curve describes this relationship: as the EESC increases the efficiency of volcanic halogen ozone depletion decreases (Figure 11). This relationship suggests that column ozone is most sensitive to volcanic halogens when the additional EESC is < 20 Tg, and that increasing the volcanic EESC flux beyond 60 Tg has little impact on column ozone change. This analysis spans simulations with very different background EESC and column ozone values. Wade et al. (2020), Brenna et al. (2019), and Brenna et al. (2020) simulations are all in a pre-industrial atmosphere background states with low background chlorine levels, whereas, the background chlorine levels in HAL10 and HAL56 are significantly higher and with lower initial ozone columns. This relationship suggests that the peak global-mean ozone loss (%) is dependent more on the volcanically injected EESC than the background chlorine and initial ozone columns. In other words, this relationship is time-independent and this exponential decay curve can be used to estimate the peak global-mean ozone loss for an eruption in any climate state, including future eruptions where the background EESC will have decayed back to pre-1980s levels. This will be especially useful for rapid estimates of ozone change as new or better constrained volcanic halogen data becomes available.

https://doi.org/10.5194/acp-2020-1110
Preprint. Discussion started: 6 November 2020

Atmospheric Chemistry and Physics Discussions

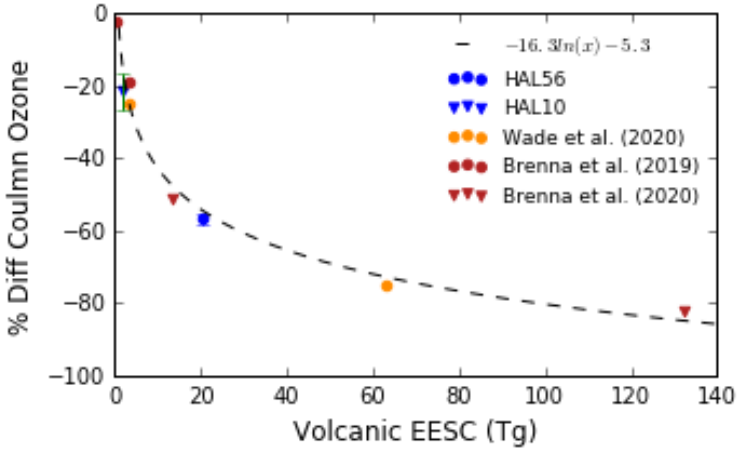

450

Figure 11 Relationship between volcanically emitted EESC (Cl + 60*Br (Tg)) and peak global-mean % difference in column ozone. Blue : HAL10 and HAL56 ensemble mean and range. Green : Wade et al., 2020 ensemble mean. Red : Brena et al., 2019 and 2020 ensemble mean.

455 The implications of ozone depletion in HAL10 and HAL56 go further than enhancing the $ERF_{clear,clean}$. High anthropogenic fluxes of halocarbons into the atmosphere during the 1980s caused background chlorine levels to be elevated during the 1990s and an ozone hole is simulated to develop in the polar region every SH winter (Figure S4) of our control simulation. Using the definition for ozone hole conditions as <220 DU, we simulate enhanced ozone hole conditions following both HAL10 and HAL56 eruptions (Figure 12). In HAL10, ozone hole conditions
460 are simulated in the tropics for one year after the eruption, and a deepening of ozone hole conditions is seen in northern hemisphere polar regions for two and in the southern hemisphere polar regions for four winters. In HAL56, we simulate ozone hole conditions globally for 5 years, continuing for a further three winters in the NH polar regions and six winters in the SH polar regions.

https://doi.org/10.5194/acp-2020-1110
Preprint. Discussion started: 6 November 2020

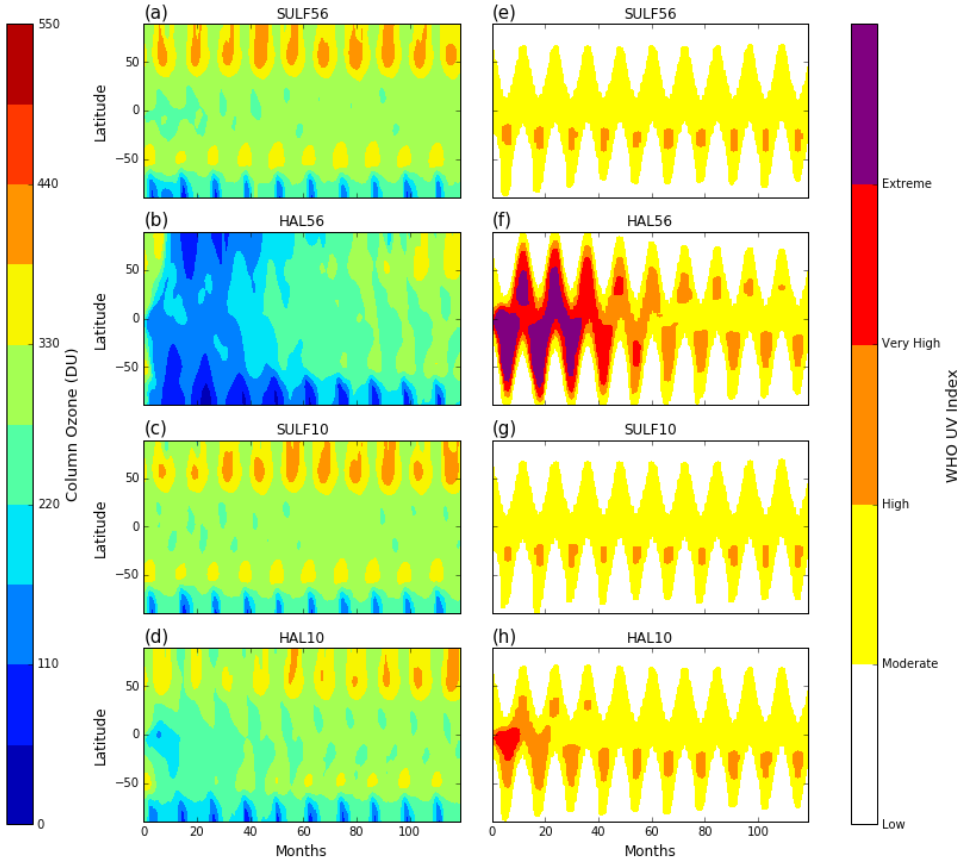

Figure 12 Zonal mean column ozone **(a)** SULF56, **(b)** HAL56, **(c)** SULF10, **(d)** HAL10. Ozone hole conditions are simulated when the column ozone < 220 DU. Zonal mean surface UV exposure due to column ozone change (WHO UV Index) **(e)** SULF56, **(f)** HAL56, **(g)** SULF10, **(h)** HAL10.

Column ozone depletion on this scale would dramatically increase the flux of harmful UV to the surface, which could cause DNA damage to animals and plants, and increase the occurrences of skin cancers, eye damage and immune system deficiencies among the population (WHO, 2017). Climate modeling and environmental proxies showed that ozone depletion as a result of halogen degassing during the emplacement of Siberian Traps flood basalts lead to ozone depletion that stressed ecosystems and caused DNA mutations which may have contributed to the end-Permian mass extinction (Black et al., 2014). A simple heuristic relating column ozone to clear-sky surface UV index is given by:

$$UV\ Index\ =\ 12.5\mu_o^{2.42}(\Omega/300)^{-1.23}$$

https://doi.org/10.5194/acp-2020-1110
Preprint. Discussion started: 6 November 2020

as defined in Madronich (2007), where μ_o is the cosine of the solar zenith angle and Ω is the total vertical ozone column in Dobson units. The monthly mean average UV index coloured by World Health Organization categories (Low [0 to 2], Medium [3 to 5], High [6 to 7], Very High [8 to 10], and Extreme [11+]) is shown in Figure 12. This shows that in the HAL56 scenario, on average 'Very High' or 'Extreme' UV levels would be expected all day for much of the globe in the three to four summers after the eruption, with noon values being even higher. Living under such a high UV exposure would cause immediate immunosuppression, epidemic outbreaks, increases in the occurrences of eye damage and, in the longer term, skin cancers among the population living between the equator and the mid-latitudes, which equates to >95% of the global population. It is worth noting, that the assessment of surface UV changes is made more challenging by the presence of volcanic aerosols, which also scatter UV radiation. However, damaging UVB and UVC radiation will not be scattered effectively by larger aerosol size distributions and volcanic aerosol levels reduce rapidly after peaking in the first post eruption year.

Whilst we have been able to calculate the composition and climate impacts of the co-emission of halogens and SO_2 from volcanic eruptions, these calculations are not without some uncertainty. Recent studies carried out as part of the Volcanic Forcings Model Intercomparison Project (VolMIP) showed large model response disparities in simulations of SO_2-only volcanic eruptions (Clyne et al., in review), but models have been shown to capture the effects of ozone depleting substances on stratospheric ozone well (WMO, 2014). As outlined in the introduction, the major uncertainty in this work is the stratospheric injection of HCl and HBr from explosive volcanic eruptions, which is highly variable and depends on both the geochemistry of the volcano and the degree of scavenging determined by the prevailing atmospheric conditions during the eruption. It is clear, however, that significant stratospheric halogen fluxes occur after some explosive volcanic eruptions.

Although this work has focused on simulations of explosive volcanic eruptions in a background climate representative of the 1990s, Figure 11 demonstrates the simulated ozone depletion predominantly depends on the volcanic halogen injection size and not the background atmospheric state. Using the relationship outlined in Figure 11, we can estimate the peak global-mean ozone percentage loss for any size of volcanic halogen injection, past or present. We plan to explore this more and understand the impacts that plausible future background atmospheric states (such as different greenhouse gas concentrations, background halogen levels and stratospheric temperatures) may have on the simulated ozone response and volcanic ERF due to co-emitted sulfur and halogen volcanic emissions.

In addition to the co-emission of volcanic halogens, there is also scope to model the co-emission of volcanic water vapour and ash directly into the stratosphere. LeGrande et al., 2016, provided a mechanism explaining how SWV originating from volcanic eruptions may alter the chemistry of the stratosphere and the nucleation rate of sulfate aerosol, and suggested that this may severely alter the climate impacts. In addition, SVW proved to be an amplifying feedback in simulations in this work and it would be interesting to see how co-emission of water vapour, halogens and sulfur would further alter the volcanic forcing in simulations of explosive volcanic eruptions. Zhu et al., 2020, showed the importance of including volcanic ash injections in climate simulations. When heterogeneous chemistry on ash particles was included they found that 43% more volcanic sulfur was removed

https://doi.org/10.5194/acp-2020-1110
Preprint. Discussion started: 6 November 2020


Atmospheric Chemistry and Physics Discussions

from the stratosphere in the first 2 months. Volcanic ash is also likely to alter the lifetime, activation and impact of co-emitted volcanic halogens in climate simulations.

5 Conclusions

In this study we utilised UKESM-AMIP simulations of volcanic eruptions to investigate how the co-emission of volcanic halogens and sulfur alters the effective radiative forcing (ERF) of explosive volcanic eruptions under atmospheric conditions representative for the mid-1990s. As the volcanic flux of HCl and HBr into the stratosphere remains uncertain, a range of plausible explosive volcanic emissions scenarios based on petrological degassing estimates, satellite observations and volcanic plume modelling were simulated. The four sets of experiments included one high SO_2 (56 Tg), and one low SO_2 (10 Tg) emission scenario, both with (HAL56 and HAL10) and without halogens (SULF56 and SULF10), each with an ensemble size of 6 sampling different QBO states. These eruption sizes (56 and 10 Tg SO_2) are similar in size to a VEI 7 (e.g. 1257 Mt. Samalas) and VEI 6 (e.g. 1991 Mt. Pinatubo) eruption, representing 1 in 500 -1000 year and 1 in 50-100 year events respectively. HAL56 utilises the 1257 Mt. Samalas HCl and HBr emission estimates from Vidal et al. (2014) and assumes a conservative ~5% stratospheric halogen injection efficiency. HAL10 has a SO_2 injection similar to 1991 Pinatubo and a 10 times smaller injection of HCl and HBr than HAL56.

We have shown that the co-emission of halogens and sulfur in simulations of explosive volcanic eruptions increases the peak and cumulative volcanic ERF significantly. This is due to a combination of increased forcing from i) volcanic aerosol-radiation interactions (ERF_{ari}) and ii) composition of the stratosphere ($ERF_{clear,clean}$).

Co-emitting halogens results in a larger global-mean ERF_{ari} in both HAL10 (+8%) and HAL56 (+6%). Ozone depletion catalysed by volcanic halogens leads to stratospheric cooling (HAL10 ≃ -2 K, HAL56 ≃ -3.5 K) which more than offsets the volcanic aerosol heating (SULF10 ≃ 1.5 K, SULF56 ≃ 3.5 K). The ozone induced stratospheric cooling prevents aerosol self-lofting and keeps the volcanic aerosol lower in the stratosphere with a shorter lifetime, resulting in reduced growth via condensation and coagulation and smaller peak global-mean effective radius compared to sulfur-only simulations. The peak global-mean effective radii of the HAL10 and HAL56 sulfate aerosols are found to be 15% and 10% smaller than SULF10 and SULF56 sulfate aerosol, closer to the most efficient radii for radiation scattering per unit mass, ~0.25 μm. Subsequently, we find HAL10 and HAL56 have higher peak global-mean SAOD anomalies (+11%, +22%) and ERF_{ari} (+8% + 6%).

Co-emission of halogens also results in significant perturbations to the stratospheric chemistry and compositional-driven forcing. Stratospheric methane was found to decrease by 3% and 18% and stratospheric water vapour (SWV) was found to reduce by 16% and 36% in HAL10 and HAL56 respectively. The methane reductions were driven by the enhanced destruction flux by volcanic Cl radicals and the SWV changes were attributed to the same stratospheric temperature reductions mentioned previously. Cooling in the tropical tropopause vicinity increased the efficiency of the tropical cold trap dehydration effect, reducing the flux of water vapour being transported from the troposphere. The most dramatic change in chemistry was found to be in stratospheric ozone. Significant ozone depletions were simulated globally in both HAL10 (22%) and HAL56 (57%) with prolonged depletion in both NH and SH winter polar regions. In HAL10, ozone hole conditions (<220 DU) were simulated globally for

https://doi.org/10.5194/acp-2020-1110
Preprint. Discussion started: 6 November 2020

Atmospheric Chemistry and Physics Discussions

the first post eruption year and then for 3-5 years at the poles during the winter. In HAL56, we simulate an ozone hole globally for 5 years followed by a gradual recovery over the following five years until only the polar winters exhibit ozone hole conditions. Stratospheric chemistry changes resulting from the co-emission of halogens increase the peak global-mean $ERF_{clear,clean}$ by ~100% to -2.1 Wm^{-2} in HAL56 and -1.3 Wm^{-2} in HAL10. Stratospheric ozone depletion is the dominant driver of $ERF_{clear,clean}$ accounting for ~75% of the total $ERF_{clear,clean}$.

The total effect of the increased ERF_{ari} and $ERF_{clear,clean}$ is that co-emitting halogens increases the peak global-mean volcanic ERF by 30% and 24% and cumulative ERF by 60% and 100% in HAL10 and HAL56 respectively. Ozone hole conditions exhibited by both HAL10 and HAL56 would result in dramatic increases in the surface UV flux with 'Extreme' UV levels being experienced over most of the globe for 4 years following HAL56 eruptions. UV exposure on this scale would lead to devastating negative consequences for society and the biosphere, including increases in the occurrences of skin cancer, eye damage and immune system deficiencies (WHO, 2002). This work shows for the first time that co-emission of plausible amounts of halogens can amplify the effective radiative forcing in simulations of explosive volcanic eruptions. This highlights the need to include volcanic halogens fluxes when simulating the climate impacts of past or future eruptions, and provides motivation to better quantify the degassing budgets and stratospheric injection estimates for volcanic eruptions.

Data Availability

All data required to reproduce our key results will be archived in the Centre for Environmental Data Analysis (CEDA) archive. Post-processing and visualization of data was performed with Python. The scripts and the post-processed data files are available on request from the corresponding author.

Author Contributions

J.SS designed the study, ran the UKESM1-AMIP experiments, analyzed the results and wrote the manuscript. A.S. and A.A. provided support for designing the study and analyzing the results. T.A., Y.M.S, J.W., L.R.M., N.L.A. provided support for running the experiments, and T.A., Y.M.S, J.W., provided support for the analysis. All authors contributed to revising the manuscript.

Competing interests.

The authors declare that they have no conflict of interests.

Acknowledgements

JSS and YMS would like to thank NERC through the University of Cambridge ESS-DTP for funding; JW would like to thank the Cambridge Commonwealth, European & International Trust for funding through a Vice Chancellor's Award. T.J.A. acknowledges support from the Royal Society through a Newton International Fellowship (grant number NIF\R1\180809), from the European Union's Horizon 2020 research and innovation programme under the Marie Skłodowska-Curie grant agreement No 835939, and from the Sidney Sussex college

https://doi.org/10.5194/acp-2020-1110
Preprint. Discussion started: 6 November 2020

Atmospheric Chemistry and Physics Discussions

through a Junior Research Fellowship. L.R.M. and A.S. are funded by the U.K. Natural Environment Research Council (NERC) via the "Vol-Clim" grant (NE/S000887/1). We would like to thank NERC, through NCAS, and the Met Office for the support of the JWCRP UKCA project. NLA and ATA are supported by NERC and NCAS through the ACSIS project. The team thank NCAS and the Met Office, through the JWCRP, for support of the UKCA model. This work used Monsoon2, a collaborative High Performance Computing facility funded by the Met Office and the Natural Environment Research Council. This work used JASMIN, the UK collaborative data analysis facility.

References

Archibald, A. T., O'Connor, F. M., Abraham, N. L., Archer-Nicholls, S., Chipperfield, M. P., Dalvi, M., Folberth, G. A., Dennison, F., Dhomse, S. S., Griffiths, P. T., Hardacre, C., Hewitt, A. J., Hill, R. S., Johnson, C. E., Keeble, J., Köhler, M. O.,

B. A. Black, J.-F. Lamarque, C. A. Shields, L. T. Elkins-Tanton, J. T. Kiehl, Acid rain and ozone depletion from pulsed Siberian traps magmatism. Geology 42, 67–70 (2014).

Brenna, H., Kutterolf, S., and Krüger, K.: Global ozone depletion and increase of UV radiation caused by pre-industrial tropical volcanic eruptions, Sci. Rep.-UK, 9, 1–14, https://doi.org/10.1038/s41598-019-45630-0, 2019.

Brenna, H., Kutterolf, S., Mills, M. J., and Krüger, K.: The potential impacts of a sulfur- and halogen-rich supereruption such as Los Chocoyos on the atmosphere and climate, Atmos. Chem. Phys., 20, 6521–6539, https://doi.org/10.5194/acp-20-6521-2020, 2020.

Cadoux, A., B. Scaillet, S. Bekki, C. Oppenheimer, and T. H. Druitt (2015), Stratospheric ozone destruction by the Bronze-Age Minoan eruption (Santorini Volcano, Greece), Sci. Rep., 5, 12243, doi:10.1038/srep12243.

Carn, S. A., L. Clarisse, and A. J. Prata (2016), Multi-decadal satellite measurements of global volcanic degassing, J. Volcanol. Geotherm. Res.,311, 99–134, doi:10.1016/j.jvolgeores.2016.01.002.

Dhomse, S. S., Emmerson, K. M., Mann, G. W., Bellouin, N., Carslaw, K. S., Chipperfield, M. P., Hommel, R., Abraham, N. L., Telford, P., Braesicke, P., Dalvi, M., Johnson, C. E., O'Connor, F., Morgenstern, O., Pyle, J. A., Deshler, T., Zawodny, J. M., and Thomason, L. W.: Aerosol microphysics simulations of the Mt.~Pinatubo eruption with the UM-UKCA composition-climate model, Atmos. Chem. Phys., 14, 11221–11246, https://doi.org/10.5194/acp-14-11221-2014, 2014.

Eyring, V., Bony, S., Meehl, G. A., Senior, C. A., Stevens, B., Stouffer, R. J., & Taylor, K. E. (2016). Overview of the Coupled Model Intercomparison Project Phase 6 (CMIP6) experimental design and organization. Geoscientific Model Development, 9(5), 1937–1958. https://www.geosci-model-dev.net/9/1937/2016/

https://doi.org/10.5194/acp-2020-1110
Preprint. Discussion started: 6 November 2020

630 Ghan, S. J. (2013). Technical note: Estimating aerosol effects on cloud radiative forcing. Atmospheric Chemistry and Physics, 13(19), 9971– 9974. https://doi.org/10.5194/acp-13-9971-2013

Gerlach, T. M., Westrich, H. R. & Symonds, R. B. Preeruption Vapor in Magma of the Climactic Mount Pinatubo Eruption: Source of the Giant Stratospheric Sulfur Dioxide Cloud. In Newhall, C. G. & Punongbayan, C. G. (eds)
635 Fire Mud Eruptions lahars Mt. Pinatubo, Philipp. 415–433 (University of Washington Press, 1996).

Halmer, M. M., Schmincke, H.-U., & Graf, H.-F. (2002). The annual volcanic gas input into the atmosphere, in particular into the stratosphere: A global data set for the past 100 years. Journal of Volcanology and Geothermal Research, 115(3), 511–528

640

Hunton, D. E., et al. (2005), In-situ aircraft observations of the 2000 Mt. Hekla volcanic cloud: Composition and chemical evolution in the Arctic lower stratosphere, J. Volcanol. Geotherm. Res., 145, 23–34, doi:10.1016/j.jvolgeores.2005.01.005.

645

Iglesias-Suarez, F., Kinnison, D. E., Rap, A., Maycock, A. C., Wild, O., and Young, P. J.: Key drivers of ozone change and its radiative forcing over the 21st century, Atmos. Chem. Phys., 18, 6121–6139, https://doi.org/10.5194/acp-18-6121-2018, 2018.

650 Klobas, J. E., Wilmouth, D. M., Weisenstein, D. K., Anderson, J. G., and Salawitch, R. J.: Ozone depletion following future volcanic eruptions, Geophys. Res. Lett., 44, 7490–7499, https://doi.org/10.1002/2017GL073972, 2017.

Krüger, K., Kutterolf, S., and Hansteen, T. H.: Halogen release from Plinian eruptions and depletion of
655 stratospheric ozone, in: Volcanism and Global Environmental Change, edited by: Schmidt, A., Fristad, K. E., and Elkins-Tanton, L. T., 244–259, Cambridge University Press, Cambridge, 2015.

Kutterolf, S., Hansteen, T. H., Appel, K., Freundt, A., Kruger, K., Perez, W., and Wehrmann, H.: Combined bromine and chlorine release from large explosive volcanic eruptions: A threat to stratospheric ozone?, Geology,
660 41, 707–710, https://doi.org/10.1130/G34044.1, 2013.

Kutterolf, S., Hansteen, T. H., Freundt, A., Wehrmann, H., Appel, K., Krüger, K., and Pérez, W.: Bromine and chlorine emissions from Plinian eruptions along the Central American Volcanic Arc: From source to atmosphere, Earth Planet. Sc. Lett., 429, 234–246, https://doi.org/10.1016/j.epsl.2015.07.064, 2015.

665

Löffler, M. 2015, Impact of major volcanic eruptions on stratospheric water vapour, Masters Thesis, Ostbayerische Technische Hochschule, Regensburg, Germany.

Löffler, M., Brinkop, S., and Jöckel, P.: Impact of major volcanic eruptions on stratospheric water vapour, Atmos. Chem. Phys., 16, 6547–6562, https://doi.org/10.5194/acp-16-6547-2016, 2016.

Lurton, T., Jégou, F., Berthet, G., Renard, J.-B., Clarisse, L., Schmidt, A., Brogniez, C., and Roberts, T. J.: Model simulations of the chemical and aerosol microphysical evolution of the Sarychev Peak 2009 eruption cloud compared to in situ and satellite observations, Atmos. Chem. Phys., 18, 3223–3247, https://doi.org/10.5194/acp-18-3223-2018, 2018.

McCormick, P. M., Thomason, L. W. & Trepte, C. R. Atmospheric effects of the Mt Pinatubo eruption. Nature 373, 399–404 (1995).

Madronich, S. (2007). Analytic Formula for the Clear-sky UV Index. Photochemistry and Photobiology, 83(6):1537–1538.

Mankin, W. G., and M. T. Coffey (1984), Increased stratospheric hydrogen chloride in the El Chichón cloud, Science, 226, 170–173, doi:10.1126/science.226.4671.170.

Mankin, W. G., M. T. Coffey, and A. Goldman (1992), Airborne observations of SO_2, HCl, and O_3 in the stratospheric plume of the Pinatubo volcano in July 1991, Geophys. Res. Lett., 19, 179–182, doi:10.1029/91GL02942.

Ming, A., Winton, V. H. L., Keeble, J.,Abraham, N. L., Dalvi, M. C., Griffiths, P., et al. (2020). Stratospheric ozone changes from explosive tropical volcanoes: Modeling and ice core constraints. Journal of Geophysical Research: Atmospheres, 125, e2019JD032290. https://doi.org/10.1029/2019JD032290

Morgenstern, O., Mulcahy, J. P., Ordóñez, C., Pope, R. J., Rumbold, S. T., Russo, M. R., Savage, N. H., Sellar, A., Stringer, M., Turnock, S. T., Wild, O., and Zeng, G.: Description and evaluation of the UKCA stratosphere–troposphere chemistry scheme (StratTrop vn 1.0) implemented in UKESM1, Geosci. Model Dev., 13, 1223–1266, https://doi.org/10.5194/gmd-13-1223-2020, 2020.

Mulcahy, J. P., Johnson, C., Jones, C. G., Povey, A. C., Scott, C. E., Sellar, A., Turnock, S. T., Woodhouse, M. T., Abraham, N. L., Andrews, M. B., Bellouin, N., Browse, J., Carslaw, K. S., Dalvi, M., Folberth, G. A., Glover, M., Grosvenor, D., Hardacre, C., Hill, R., Johnson, B., Jones, A., Kipling, Z., Mann, G., Mollard, J., O'Connor, F. M., Palmieri, J., Reddington, C., Rumbold, S. T., Richardson, M., Schutgens, N. A. J., Stier, P., Stringer, M., Tang, Y., Walton, J., Woodward, S., and Yool, A.: Description and evaluation of aerosol in UKESM1 and HadGEM3-GC3.1 CMIP6 historical simulations, Geosci. Model Dev. Discuss., https://doi.org/10.5194/gmd-2019-357, 2020.

Newhall, C., Self, S., Robock A.; Anticipating future Volcanic Explosivity Index (VEI) 7 eruptions and their chilling impacts. Geosphere ; 14 (2): 572–603. doi: https://doi.org/10.1130/GES01513.1

https://doi.org/10.5194/acp-2020-1110
Preprint. Discussion started: 6 November 2020

710 Osprey, S. M., Gray, L. J., Hardiman, S. C., Butchart, N., & Hinton, T. J. (2013). Stratospheric variability in twentieth-century CMIP5 simulations of the MET office climate model: High top versus low top. Journal of Climate, 26(5), 1595–1606. ttps://doi.org/10.1175/JCLI-D-12-00147.1

Prata, A. J., S. A. Carn, A. Stohl, and J. Kerkmann (2007), Long range transport and fate of a stratospheric volcanic
715 cloud from Soufrière Hills volcano, Montserrat, Atmos. Chem. Phys., 7, 5093– 5103, doi:10.5194/acp-7-5093-2007

Rap, A., Richards, N. A. D., Forster, P. M., Monks, S. A., Arnold, S. R., and Chipperfield, M. P.: Satellite constraint on the tropospheric ozone radiative effect, Geophys. Res. Lett., 42, 5074– 5081,
720 https://doi.org/10.1002/2015GL064037, 2015.

Read, W. G., L. Froidevaux, M. L. Santee, and N. J. Livesey (2009), Observations of volcanic SO2 and HCl from Aura MLS, AGU, Fall Meeting 2009.

725 Robock, A. Volcanic eruptions and climate. Rev. Geophys. 45, 191–219 (2000)

Rose, W. I., et al. (2006), Atmospheric chemistry of a 33–34 hour old volcanic cloud from Hekla Volcano (Iceland): Insights from direct sampling and the application of chemical box modeling, J. Geophys. Res., 111, D20206, doi:10.1029/2005JD006872.

730

Sellar, Alistair & Walton, Jeremy & Jones, Colin & Wood, Richard & Abraham, Nathan & Andrejczuk, M. & Andrews, Martin & Andrews, Timothy & Archibald, Alex & Mora, Lee de & Dyson, Harold & Elkington, Mark & Ellis, Rich & Florek, Piotr & Good, Peter & Gohar, L. & Haddad, Stephen & Hardiman, Steven & Hogan, Emma & Wiltshire, Andy. (2020). Implementation of UK Earth system models for CMIP6. Journal of Advances
735 in Modeling Earth Systems. 12. 10.1029/2019MS001946.

Sellar, A. A., Jones, C. G., Mulcahy, J., Tang, Y., Yool, A., Wiltshire, A., O'Connor, F. M., Stringer, M., Hill, R., Palmieri, J., Woodward, S., de Mora, L., Kuhlbrodt, T., Rumbold, S. T., Kelley, D. I., Ellis, R., Johnson, C. E., Walton, J., Abraham, N. L., Andrews, M. B., Andrews, T., Archibald, A. T., Berthou, S., Burke, E., Blockley, E.,
740 Carslaw, K., Dalvi, M., Edwards, J., Folberth, G. A., Gedney, N., Griffiths, P. T., Harper, A. B., Hendry, M. A., Hewitt, A. J., Johnson, B., Jones, A., Jones, C. D., Keeble, J., Liddicoat, S., Morgenstern, O., Parker, R. J., Predoi, V., Robertson, E., Siahaan, A., Smith, R. S., Swaminathan, R., Woodhouse, M. T., Zeng, G., Zerroukat, M., & Zerroukat, M. (2019). UKESM1: Description and evaluation of the UK Earth System Model. Journal of Advances in Modeling Earth Systems, 11, 4513– 4558. https://doi.org/10.1029/2019MS001739

745

Self, S. et al. in Fire and Mud: Eruptions and lahars of Mount Pinatubo, Philippines (eds Newhall, C. G. & Punongbayan, R. S.) 1089–1115 (University of Washington Press, 1996).

https://doi.org/10.5194/acp-2020-1110
Preprint. Discussion started: 6 November 2020

Atmospheric Chemistry and Physics Discussions

Schmidt, A., Mills, M. J., Ghan, S., Gregory, J. M., Allan, R. P., Andrews, T., Bardeen, C. G., Conley, A., Forster, P. M., Gettelman, A., Portmann, R. W., Solomon, S., & Toon, O. B. (2018). Volcanic radiative forcing from 1979 to 2015. Journal of Geophysical Research: Atmospheres, 123, 412– 491. https://doi.org/10.1029/2018JD028776

Solomon, S. (1999). Stratospheric ozone depletion: A review of concepts and history. Reviews of Geophysics, 37(3), 275–316. https://doi.org/10.1029/1999RG900008

Telford, P. J., Abraham, N. L., Archibald, A. T., Braesicke, P., Dalvi, M., Morgenstern, O., et al. (2013). Implementation of the fast-JX photolysis scheme (v6.4) into the UKCA component of the MetUM chemistry-climate model (v7.3). Geoscientific Model Development, 6(1), 161–177. https://www.geosci-model-dev.net/6/161/2013/

Textor, C., H.-F. Graf, M. Herzog, and J. M. Oberhuber (2003), Injection of gases into the stratosphere by explosive volcanic eruptions, J. Geophys. Res., 108(D19), 4606, doi:10.1029/2002JD002987.

Theys, N., De Smedt, I., Van Roozendael, M., Froidevaux, L., Clarisse, L., & Hendrick, F. (2014). First satellite detection of volcanic OCLO after the eruption of Puyehue-Cordòn Caulle. Geophysical Research Letters, 41, 667–672. https://doi.org/10.1002/2013GL058416

Tie, X., and G. Brasseur (1995), The response of stratospheric ozone to volcanic eruptions: Sensitivity to atmospheric chlorine loading,Geophys. Res. Lett., 22, 3035–3039, doi:10.1029/95GL03057.

Varekamp, J. C., Luhr, J. F. & Prestegaard, K. F. The 1982 eruption of El Chichon volcano (Chiapas, Mexico): character of the eruptions, ash-fall deposits and gas phase. J. Volcanol. Geotherm. Res. 23, 39–68 (1984).

Vidal, C. M., Métrich, N., Komorowski, J.-C., Pratomo, I., Michel, A., Kartadinata, N., et al. (2016). The 1257 Samalas eruption (Lombok, Indonesia): The single greatest stratospheric gas release of the Common Era. Scientific reports, 6, 34,868. https://doi.org/10.1038/ srep34868

Wade, D. C., Vidal, C.M., Abraham, N. L., Dhomse, S., Griffiths, P. T., Keeble, J., Mann, G., Marshall, L., Schmidt, A., Archibald, A. T., (2020). Reconciling the climate and ozone response to the 1257 CE Mount Samalas eruption. Proceedings of the National Academy of Sciences Oct 2020, 201919807; DOI: 10.1073/pnas.1919807117

Wallace, L., & Livingston, W. (1992). The effect of the Pinatubo cloud on hydrogen chloride and hydrogen fluoride. Geophysical Research
Letters, 19(12), 1209–1209. https://doi.org/10.1029/92GL01112

https://doi.org/10.5194/acp-2020-1110
Preprint. Discussion started: 6 November 2020

Westrich, H. R., and T. M. Gerlach (1992), Magmatic gas source for the stratospheric SO2 cloud from the June 15, 1991, eruption of Mount Pinatubo, Geology, 20, 867–870, doi:10.1130/0091-7613(1992)020<0867:MGSFTS>2.3.CO;2.

Woods, A. W., Chuan, R. L. & Rose, W. I. Halite particles injected into the stratosphere by the 1982 El Chichón eruption. Science (80-.) 230, 170–172 (1985).

WMO: Scientific Assessment of Ozone Depletion: 2018, Geneva, Switzerland, 2018.

World Meteorological Organization (WMO) (2014) Scientific assessment of ozone depletion: 2014, global ozone research and monitoring project—report no. 55, Geneva, Switzerland, p 416

Zdanowicz, C. M., G. A. Zielinski, and M. S. Germani (1999), Mount Mazama eruption: Calendrical age verified and atmospheric impact assessed, Geology, 27, 621–624, doi:10.1130/0091-7613(1999)027<0621:MMECAV>2.3.CO;2.